2012

A single amino acid change resulting in loss of fluorescence of eGFP in a viral fusion protein confers fitness and growth advantage to the recombinant vesicular stomatitis virus

Phat X. Dinh
University of Nebraska-Lincoln, s-pdinh3@unl.edu

Debasis Panda
University of Nebraska - Lincoln, dpanda2@unl.edu

Phani B. Das
University of Nebraska-Lincoln, pdas2@unl.edu

Subash C. Das
University of Nebraska - Lincoln, sdas2@unl.edu

Anshuman Das
University of Nebraska-Lincoln, adas2@unl.edu
See next page for additional authors

Virology 432 (2012) 460–469

Contents lists available at SciVerse ScienceDirect

Virology

journal homepage: www.elsevier.com/locate/yviro

A single amino acid change resulting in loss of fluorescence of eGFP in a viral fusion protein confers fitness and growth advantage to the recombinant vesicular stomatitis virus

Phat X. Dinh [a,b], Debasis Panda [a,b,1], Phani B. Das [a,b,2], Subash C. Das [a,b,3], Anshuman Das [a,b], Asit K. Pattnaik [a,b,*]

[a] School of Veterinary Medicine and Biomedical Sciences, University of Nebraska-Lincoln, Lincoln, Nebraska 68583-0900, USA
[b] The Nebraska Center for Virology, University of Nebraska-Lincoln, Lincoln, Nebraska 68583-0900, USA

ARTICLE INFO

Article history:
Received 29 April 2012
Returned to author for revisions
25 May 2012
Accepted 3 July 2012
Available online 24 July 2012

Keywords:
VSV
PeGFP fusion protein
Dual-fluorescent virus
Viral fitness
Growth advantage
Transcription
Replication

ABSTRACT

Using a recombinant vesicular stomatitis virus encoding eGFP fused in-frame with an essential viral replication protein, the phosphoprotein P, we show that during passage in culture, the virus mutates the nucleotide C289 within eGFP of the fusion protein PeGFP to A or T, resulting in R97S/C amino acid substitution and loss of fluorescence. The resultant non-fluorescent virus exhibits increased fitness and growth advantage over its fluorescent counterpart. The growth advantage of the non-fluorescent virus appears to be due to increased transcription and replication activities of the PeGFP protein carrying the R97S/C substitution. Further, our results show that the R97S/C mutation occurs prior to accumulation of mutations that can result in loss of expression of the gene inserted at the G–L gene junction. These results suggest that fitness gain is more important for the recombinant virus than elimination of expression of the heterologous gene.

Introduction

Vesicular stomatitis virus (VSV) is a non-segmented negative-stranded RNA virus in the family *Rhabdoviridae* and order *Mononegavirales*. It is widely used as a model pathogen for understanding of myriad aspects of biology of negative-stranded RNA viruses including viral genome transcription and replication, innate and adaptive immune responses, host responses to viral infections, viral evolution and many aspects of molecular biology of eukaryotic cells. In recent years, VSV has also been used as a viral vector for expression of heterologous genes, for vaccine development and as an oncolytic agent for specific killing of tumor cells (Barber, 2005; Geisbert et al., 2010; Heiber et al., 2011; Lichty et al., 2004).

VSV possesses a simple genomic organization with five non-overlapping genes (encoding the five structural proteins of the virion) in the order of 3′–N-P-M-G-L-5′. The N protein binds the viral genomic RNA to form a nucleocapsid template that is recognized by the viral RNA-dependent RNA polymerase (RdRp) composed of the P and L proteins, for transcription and replication of the viral genome. The M and G proteins are required for assembly and budding of infectious virus particles. Within the viral genome, each gene is flanked by highly conserved upstream transcription initiation signals and downstream transcription termination signals that dictate synthesis of monocistronic, capped, and polyadenylated viral mRNAs. Due to the modular and non-overlapping gene organization, it has been relatively straightforward to insert heterologous genes into the viral genome and recover infectious recombinant viruses. Consequently, recombinant VSV expressing heterologous proteins (Geisbert et al., 2010; Lichty et al., 2004; McKenna et al., 2003) including various proteins and antigens from other viral and bacterial sources have been used to monitor immune responses and protective immunity in vitro and in vivo.

Since the VSV RNA polymerase, like other viral RNA polymerases, lacks proof-reading activity and is error-prone, the sequence integrity and expression of the foreign genes in VSV are known to be compromised due to accumulation of mutations

* Corresponding author at: University of Nebraska-Lincoln Veterinary and Biomedical Sciences, 109 Morrison Life Science Research Center 4240 Fair Street East Campus Lincoln, Nebraska, NE 68583-0900, United States.
Fax: +1 402 472 3323.
E-mail address: apattnaik2@unl.edu (A.K. Pattnaik).
[1] Present address: Department of Microbiology, Perelman School of Medicine, University of Pennsylvania, Philadelphia, PA 19104.
[2] Present address: Department of Molecular and Cell Biology, University of California, Berkeley, 94720.
[3] Present address: Inviragen, Inc., Madison, WI 53719.

0042-6822/$ - see front matter © 2012 Elsevier Inc. All rights reserved.
http://dx.doi.org/10.1016/j.virol.2012.07.004

in these genes. Under normal conditions of selective pressure to maintain the functionality of viral proteins, the VSV polymerase introduces nucleotide substitutions in the viral genome resulting in generation of viral quasispecies that may differ from each other on the basis of growth potential and fitness (Moya et al., 2000; Steinhauer et al., 1989). The generation and characteristics of the viral quasispecies and their fitness in an infected host have been considered to be important for understanding of viral evolution and the dynamics of the viral population (Domingo et al., 2001; Elena et al., 1996; Pfeiffer and Kirkegaard, 2006; Vignuzzi et al., 2006). In addition, studies with VSV have also led to establishment and demonstration of important evolutionary principles such as the Muller's ratchet (Duarte et al., 1992; Muller, 1964), the Red Queen Hypothesis (Clarke et al., 1994; van Valen, 1973), the Competitive Exclusion Principle (Clarke et al., 1994; Gause et al., 1971), among others (Domingo et al., 2001).

The manner in which VSV evolves and gains fitness under conditions of carrying foreign genes have not been investigated in detail (Novella, 2003). How would the viral polymerase respond to heterologous sequences fused with an essential viral protein to maintain the reading frame of the essential viral protein to generate viable viruses is unclear. Expression of heterologous genes introduced at the G–L gene junction of VSV becomes extinguished through mutation(s) at the transcription termination and/or initiation sites upstream of the introduced gene or mutation(s) resulting in termination codon within the gene (Quinones-Kochs et al., 2001). Recombinant VSV encoding eGFP fused in-frame at the carboxy-terminus of the G protein, upon passage, has been shown to eliminate the expression of eGFP due to introduction of stop codon in the carboxy-terminus of the G protein (Dalton and Rose, 2001). When eGFP is inserted in-frame in the L protein, the resultant recombinant VSV becomes temperature-sensitive (Ruedas and Perrault, 2009). Although this virus was shown to be genetically stable in four passages of plaque-purified virus stocks, it grew to significantly lower titers in the fourth passage (Ruedas and Perrault, 2009), perhaps indicating accumulation of deleterious mutations in the genome of the viruses in the population.

We had previously generated a recombinant VSV (VSV-PeGFP) encoding P protein fused in-frame with eGFP sequences (Das et al., 2006). Interestingly, passaging of the virus without plaque-purification led to rapid loss of fluorescence in infected cells and generation of infectious VSV without fluorescence, whereas plaque-purified VSV-PeGFP was relatively stable for at least twenty passages in culture. Studies reported here were conducted to understand the basis for the loss of fluorescence and determine whether the loss of fluorescence imparts any growth advantage and/or fitness gain to the non-fluorescent virus. Our results identified a single nucleotide substitution (C289A/T) within the eGFP sequence, generating a non-fluorescent protein and conferring increased fitness and growth advantage to the resulting virus. To our knowledge, this is the first description of a specific nucleotide mutation in the inserted eGFP sequence that leads to fitness gain and growth advantage for the virus.

Results and discussion

A single nucleotide change (C289A/T) in eGFP coding sequence in PeGFP fusion protein of VSV-PeGFP virus results in a non-fluorescent protein

We had previously described (Das et al., 2006) recovery of a recombinant VSV (VSV-PeGFP) encoding PeGFP fusion protein in which eGFP was fused in-frame following the amino acid 196 of the viral P protein (Fig. 1A). In subsequent studies, when the virus

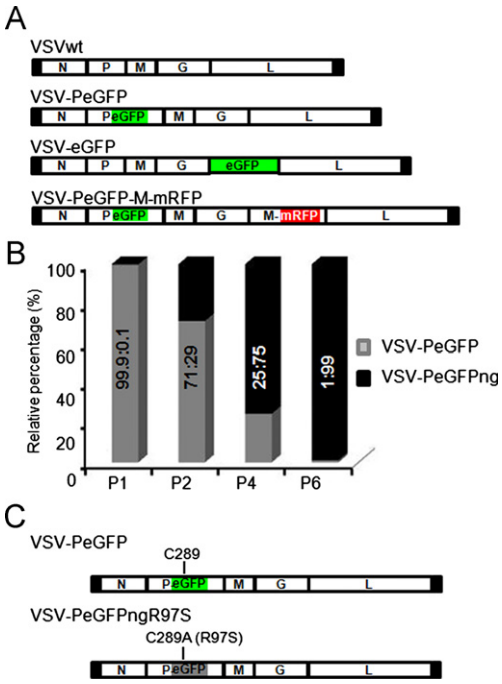

Fig. 1. Identification of a mutation within eGFP coding sequence in PeGFP fusion protein of VSV-PeGFP virus. (A) Recombinant VSV genome constructs used in this study. VSVwt, the wt VSV genome, with N, P, M, G and L shown in rectangular boxes; VSV-PeGFP, genome encoding PeGFP in place of wt P; VSV-eGFP, eGFP was inserted as an independent cistron at the G–L junction; VSV-PeGFP-M-MmRFP, genome encoding PeGFP in place of wt P and MmRFP as an extra cistron at the G–L junction. (B) Emergence and dominance of VSV-PeGFPng from the culture supernatant of plasmid recovered population of recombinant VSV-PeGFP. The supernatant containing recovered VSV-PeGFP virus (passage 0, P0) was passaged at 0.01 MOI on BHK-21 cells and the percentage of VSV-PeGFPng virus was determined by plaque assay and counting of fluorescent and non-fluorescent viruses in various passages. Histograms show the average data from three independent experiments. (C) C289A is the only mutation found in full-length genome of VSV-PeGFPngR97S compared to VSV-PeGFP virus. RNA genome of VSV-PeGFP and VSV-PeGFPngR97S viruses was isolated directly from P0 supernatant (as in B). The viral RNAs were subjected to RT-PCR, followed by nucleotide sequencing for the whole genome using the primers shown in Table 2.

recovered from the transfected culture supernatants was passaged in cells without plaque purification, we observed rapid loss of green fluorescence resulting in recombinant virus (VSV-PeGFPng) that displayed non-fluorescent [non-green (nG)] phenotype. The proportion of VSV-PeGFPng was only 0.1% at P1 but increased to about 29% in P2. By passage 6, VSV-PeGFPng represented approximately 99% of the total infectious particles (Fig. 1B) as judged by enumerating the number of fluorescent and non-fluorescent plaques in plaque assays.

To determine the molecular basis of the loss of eGFP fluorescence in the infectious particles or in infected cells, twelve non-fluorescent and four fluorescent plaques were isolated from a plaque assay of P1 culture supernatant and the virus in these plaques were amplified by passage in cells. During this passage, the monolayer of cells infected with virus from non-fluorescent plaques did not display any fluorescence while the cells infected with virus from fluorescent plaques were all fluorescing green. Both the fluorescent (VSV-PeGFP) and non-fluorescent (VSV-PeGFPng) viruses synthesized full-length PeGFP protein in infected cells and also packaged the PeGFP protein in the virions as judged by radiolabeling and analysis of the viral proteins (data not shown). The PeGFP coding region from the virus in the culture supernatant of infected cells was then reverse-transcribed and amplified by PCR and subjected to nucleotide sequencing. Although no sequence changes were detected in the PeGFP fusion protein of the viruses isolated from fluorescent plaques, the

Table 1
Mutations found in PeGFP, eGFP and MmRFP regions of VSV-PeGFP, VSV-eGFP and VSV-PeGFP-M-MmRFP viruses.

Virus	Phenotype	Mutation (amino acid change)
VSV-PeGFP*	G	None*
VSV-PeGFPng* (emerged from the transfected culture supernatant of recovered VSV-PeGFP)	nG	C289A (R97S)* or C289T (R97C) in eGFP
VSV-PeGFPng (emerged from the plaque-purified VSV-PeGFP during passaging)	nG	C289T (R97C) and G608T (S203I) in eGFP
VSV-PeGFP-M-MmRFP	GR	None
VSV-PeGFP-M-MmRFPngr	nGR	C289T (R97C) in eGFP
VSV-PeGFP-M-MmRFPgnr	GnR	G659A (W220Stop) in M of MmRFP
	GnR	$TATG(A)_7 \rightarrow TATA(A)_7$
	GnR	G148T (E50Stop) in M of MmRFP
	GnR	$TATG(A)_7 \rightarrow TAT(A)_7$
VSV-PeGFP-M-MmRFPngnr	nGnR	C289T (R97C) in eGFP and $TATG(A)_7 \rightarrow TAT(A)_7$ of MmRFP
	nGnR	C289T (R97C) in eGFP and C285A (Y95Stop) in M of MmRFP
	nGnR	C289T (R97C) in eGFP and $TATG(A)_7 \rightarrow TATGAAAAGAA$ of MmRFP
	nGnR	C289T (R97C) in eGFP and $TATG(A)_7 \rightarrow TATGACAAAAA$ of MmRFP
VSV-eGFP	G	None
VSV-eGFPng	nG	A545C (H182P) in eGFP
	nG	$TATG(A)_7 \rightarrow TATG(TAAAATA)$
	nG	$TATG(A)_7 \rightarrow TATG(TAAAAATA)$ and T656G (M219R) in eGFP
	nG	$TATG(A)_7 \rightarrow TATG(TACAATA)$ and C321A (Y107Stop) in eGFP
	nG	$TATG(A)_7 \rightarrow TATG(TACAATA)$
	nG	$TATG(A)_7 \rightarrow TATG(TAAAATA)$ and A136T (K46Stop) in eGFP
	nG	$TATG(A)_7 \rightarrow TATG(TAAAATA)$ and G184A (V62M) in eGFP

The (*) indicates the viruses used for full-length genome sequence determination and for competition assays.

PeGFP coding region in the plaque-purified VSV-PeGFPng viruses contained only a single nucleotide substitution (C289A) resulting in arginine to serine (R97S) change at position 97 in the eGFP sequence of the fusion protein (Table 1). Interestingly, only the same mutation was also found in VSV-PeGFPng virus from later passages (P5 and P6) indicating that the mutation is stable and rendered the PeGFP fusion protein non-fluorescent.

Results from studies using a virus with a different genomic background also supported the above contention. The recombinant VSV (VSV-PeGFP-M-MmRFP, Fig. 1A) encodes PeGFP in place of P and MmRFP (a fusion protein containing monomeric RFP fused in-frame at the carboxy-terminus of the viral M protein) at the G–L gene junction (Das et al., 2009). Majority of the recombinant VSV-PeGFP-M-MmRFP from plasmid-transfected supernatant exhibited both fluorescences (green due to PeGFP and red due to MmRFP) in infected cells but upon passage in culture, virus plaques exhibiting dual-fluorescence (GR), only red-fluorescence (nGR), only green-fluorescence (GnR) and no fluorescence (nGnR) appeared. Interestingly, examination of virus in at least twelve plaques that were only red-fluorescent (nGR, due to loss of green fluorescence) revealed that they contained C289T mutation in the eGFP sequence leading to R97C substitution in the protein (Table 1). Surprisingly, none of the twelve plaque-purified nGR viruses from this genomic background contained the C289A nucleotide substitution as was observed for VSV-PeGFPng virus.

Since we observed C289T mutation in all the plaque-purified VSV-PeGFP-M-MmRFPngr viruses and C289A mutation in all the plaque-purified VSV-PeGFPng viruses, we investigated whether this C289A/T mutation is specific and dependent on the viral genomic background. In three further independent virus recovery and passaging studies using both viruses, we observed similar pattern of loss of fluorescence with passage as shown in Fig. 1B. Sequence analyses of eight each of plaque-purified VSV-PeGFPng and VSV-PeGFP-M-MmRFPngr (only red-fluorescent) viruses from P1 and P4 culture supernatants revealed the presence of either C289A or C289T mutation in eGFP coding region of PeGFP, suggesting that C289 could be mutated to either A or T independent of the genomic background of the virus. Again, no other nucleotide substitution was detected in PeGFP coding region of these mutant viruses.

Using VSV-eGFP virus (Das et al., 2006), which contains eGFP gene at the G–L gene junction as an extra gene, similar passaging of transfected culture supernatant led to the development of non-fluorescent plaques, although only 0.01%–1% of the plaques were non-fluorescent in the supernatants of P2–P12. The overall growth of non-fluorescent VSV (VSV-eGFPng) was similar to that of the fluorescent VSV (VSV-eGFP) (data not shown). RT-PCR amplification of viral genomes isolated from at least twelve different plaques selected randomly from two different passages (P3 and P8) revealed the presence of a variety of mutations leading to the loss of green fluorescence (Table 1). However, none of these VSV-eGFPng viruses contained C289 mutation; instead they contained mutations resulting in amino acid substitution, introduction of stop codon within eGFP sequence, and/or mutation(s) in the transcription termination signal. Similar types of mutations have been detected in recombinant VSVs encoding heterologous proteins at the G–L gene junctions (Quinones-Kochs et al., 2001). It appears that C289A/T mutation resulting in R97S/C substitution in eGFP is only observed in the context of PeGFP fusion protein, which is required for VSV replication.

Thus, from multiple independent virus recovery and passaging experiments using at least two different virus genomic backgrounds, we have observed that the nucleotide C289 in eGFP coding sequence of the PeGFP is mutated to either A (transversion mutation) or T (transition mutation) resulting in amino acid substitution of R97S/C. Since transversion mutations are less frequent as compared to transition mutations (Domingo et al., 1978; Kuge et al., 1989; Schneider and Roossinck, 2000), the results suggest that the selective pressure to mutate this particular nucleotide such that the resulting protein is non-fluorescent is strong.

R97S/C mutation in eGFP confers growth advantage to VSV-PeGFPng virus

The rapid generation of VSV-PeGFPng virus with R97S/C substitution in eGFP sequence led us to investigate if the mutation conferred any growth advantage to the viruses. To examine this, we performed single step growth kinetics studies of the viruses (wt VSV, VSV-PeGFP, VSV-PeGFPngR97S, and VSV-PeGFPngR97C)

using high MOI infection. Although the kinetics of growth of the four viruses is found to be similar, VSV-PeGFP grew to titers that were about 8-fold less than the wt VSV, confirming previous observation (Das et al., 2006). On the other hand, VSV-PeGFPng viruses harboring either R97S or R97C mutation grew to comparable titers that were close to those of the wt VSV (Fig. 2A). The difference in growth potential of VSV-PeGFP and VSV-PeGFPng viruses was significant ($p < 0.01$), indicating that R97S/C substitution in eGFP sequence of PeGFP fusion protein not only rendered the protein non-fluorescent but also conferred growth advantage to the virus. Similar growth advantage was also observed for VSV-PeGFPng virus in multistep growth kinetics analysis at low MOI (Fig. 2B). Full-length genome sequence analysis revealed that the VSV-PeGFPng differed from VSV-PeGFP by the presence of only the C289A mutation (Fig. 1C). Thus, it appears that R97S/C mutation in eGFP sequence of the fusion protein confers growth advantage to the resulting viruses.

The R97 residue in eGFP (equivalent to R96 residue in GFP sequence) is known to facilitate rapid formation and stability of the eGFP chromophore consisting of residues S65-Y66-G67 (Barondeau et al., 2003; Ormo et al., 1996) and it has been shown that R96A substitution in GFP protein results in a dominant negative protein with no fluorescence (Barondeau et al., 2003). Clearly, the data presented here suggests that the loss of fluorescence in PeGFP or some structural alterations in the fusion protein due to R97S/C substitution results in a fusion protein that helps the virus grow better. Although loss of green fluorescence in viral fusion proteins have not been systematically examined during viral passages in cell culture, R97C along with several other mutations including gene truncation and deletion were detected in porcine respiratory and reproductive syndrome virus encoding eGFP fused in-frame with the viral non-structural protein 2 (Fang et al., 2008, 2006; Kim et al., 2007). It is thus possible that a properly folded chromophore of eGFP may somehow negatively affect the function of the PeGFP protein and the VSV-PeGFP virus introduces amino acid substitutions to alter or destabilize the chromophore to enhance its growth.

Increased fitness of VSV-PeGFPng over VSV-PeGFP in competition assay

Since VSV-PeGFPng virus grew to higher titers, we examined if this virus evolved by acquiring increased fitness over that of its fluorescent counterpart. Fitness studies with recombinant VSVs harboring rearranged order of P, M and G genes have revealed that growth curve comparisons are not necessarily useful in measuring the fitness of a virus, while viral fitness can be determined in direct head-to-head competition assays (Novella et al., 2004a). Thus, in order to determine if VSV-PeGFPng acquired increased fitness over VSV-PeGFP, we performed head-to-head competition assay between the two viruses. Stocks of plaque-purified VSV-PeGFP and VSV-PGFPngR97S viruses whose full-length genome sequence had been determined (Table 1) were prepared and used in these experiments. As shown in Fig. 3A, when the two viruses (VSV-PeGFP and VSV-PeGFPng) were mixed at 1:1 ratio of infectious particles and allowed to co-infect cells at the low MOI of 0.01, the ratio of non-green:green (ng:g) infectious viruses in the resulting supernatant changed from 1:1 in P0 (the starting inoculum) to 10:1 in passage 1 (P1). Upon further passage of P1 supernatant at the same low MOI of 0.01, the ratio of ng:g virus changed to 80:1, 680:1, 2300:1 and 22,000:1 in the supernatants of P2–P5 passages, respectively. These results indicate that the VSV-PeGFPng virus out-competed the VSV-PeGFP virus in co-infection experiments very efficiently and became the predominant virus in the culture quickly. By calculating the relative fitness of the two viruses and the fitness difference (Wd) value between them as described in the materials and methods, we found that the VSV-PeGFPng virus with a fitness difference value of 2.62 at P1 is more fit than the VSV-PeGFP virus.

Since fitness of a virus is also dependent on MOI (Novella et al., 2004a), we conducted a similar experiment using a high MOI of 5. Although the ratio of ng:g virus shifted from 1:1 in P0 to 16:1 in P5 supernatant (Fig. 3B), the calculated fitness difference value of 1.45 at P1 indicated that the VSV-PeGFPng is still more fit than the VSV-PeGFP virus at high MOI. It should be noted that with high MOI, the fitness difference is somewhat less and the ratios of ng:g virus is not as dramatic as those seen with low MOI passage. This is most likely due to co-infection of same cells with the two viruses and possible complementation of the less fit virus by the higher fitness virus as has been observed previously (Novella et al., 2004a). These results further show that complementation at high MOI may have somewhat overshadowed the difference in fitness between the two competing viruses as has been described earlier (Novella et al., 2004b).

It is possible that the reduced level of VSV-PeGFP and/or increased level of VSV-PeGFPng in the competition assays may also have been a result of mutation(s) in the eGFP region as seen in Fig. 1B rather than the acquisition of increased fitness of the

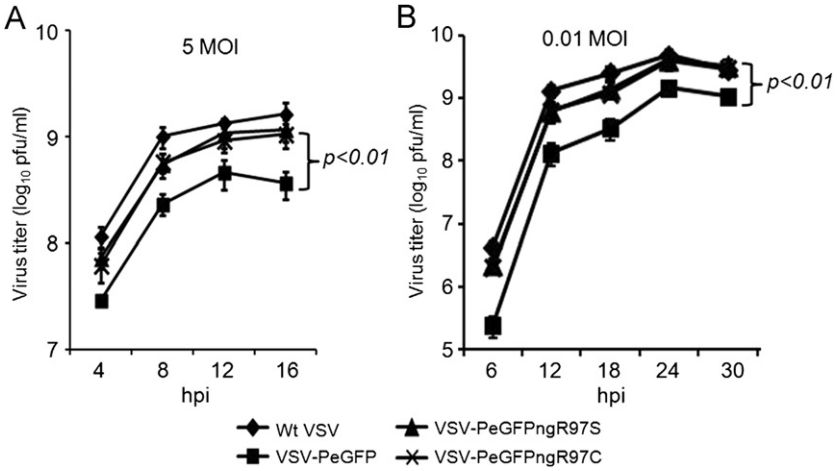

Fig. 2. R97S/C mutation in eGFP confers growth advantage to VSV-PeGFPng virus. (A) One-step growth curve of wt VSV, VSV-PeGFP, VSV-PeGFPng containing C289A (VSV-PeGFPngR97S) or C289T (VSV-PeGFPngR97C) mutation. Infection was performed in BHK-21 cells at MOI of 5, supernatants were collected at indicated time points and viral yields were determined by plaque assay in fresh BHK-21 cells. Error bars represent the standard error of mean from 3 independent experiments. (B) Multi-step growth curve. Viruses shown in A were allowed to infect BHK-21 cells separately at MOI of 0.01. Viral titers were determined and shown as described in A.

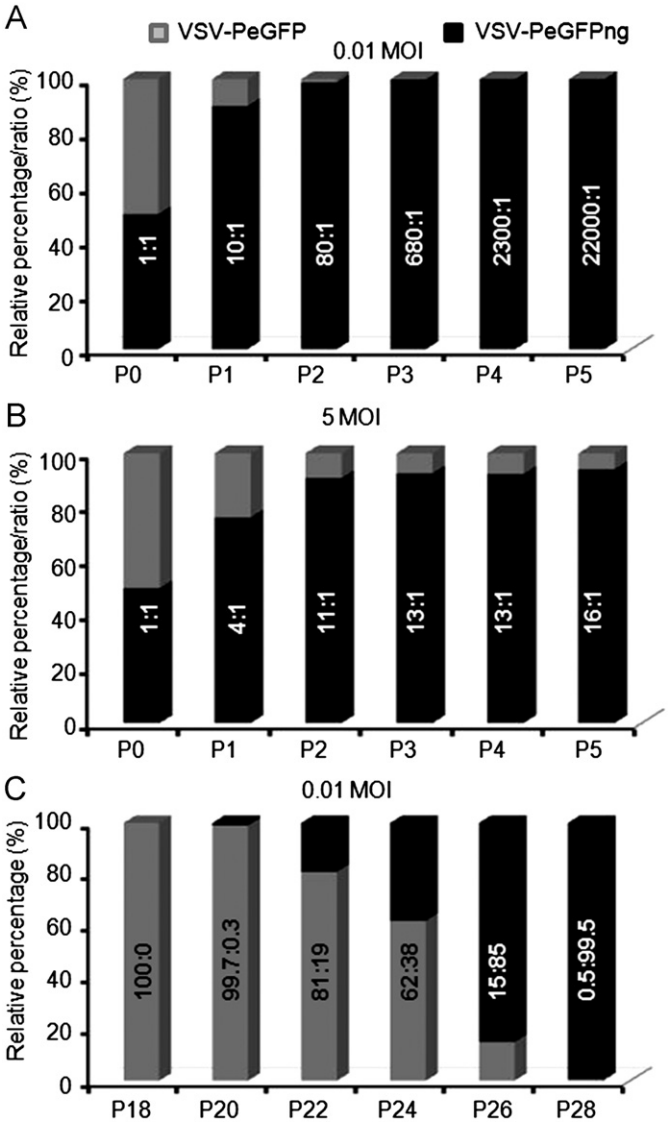

Fig. 3. Increased fitness of VSV-PeGFPng over VSV-PeGFP in competition assay. (A) Competition assay at low MOI. BHK-21 cells were co-infected at an MOI of 0.01 with a 1:1 mixture of plaque-purified VSV-PeGFP and VSV-PeGFPng (P0). At 16 hpi, supernatant (P1) was collected and titers VSV-PeGFP and VSV-PeGFPng viruses were determined in fresh BHK-21. Supernatant of P1 and subsequent passages were used to infect new BHK-21 cells at the same MOI of 0.01 to produce P2 to P5. Histograms show the average relative levels of VSV-PeGFP and VSV-PeGFPng viruses from three independent experiments. The numbers indicate the average ratio of the two viruses as determined by plaques assay in BHK-21 cells for each passage. (B) Competition assay at high MOI. The assay was done at MOI of 5 and the data were obtained as in A. (C) Kinetics of loss of green fluorescence in clonally purified VSV-PeGFP. Isolated pure green VSV-PeGFP was used to infect and passage in BHK-21 cells at MOI of 0.01. Percentage of green over non-green virus was determined as described in Fig. 1B.

VSV-PeGFPng virus. To examine if this is occurring, we used plaque-purified VSV-PeGFP and passaged at low MOI (0.01) in cells. Infectious fluorescent and non-fluorescent viruses were then enumerated by plaque assay and examination under fluorescent microscope. Examination of 500–1000 plaques at each passage did not detect any nG phenotype plaque during the first 18 passages (data not shown), indicating that the plaque-purified VSV-PeGFP is stable for at least 18 passages in culture. These results suggest that in the competition assays shown in Fig. 3A and B, the exponential increase in the number of VSV-PeGFPng virus was not due to genesis of VSV-PeGFPng from VSV-PeGFP but rather was the consequence of the better fitness and higher growth potential of the VSV-PeGFPng virus as compared to VSV-PeGFP virus. Interestingly, upon further passage of plaque-purified VSV-PeGFP, non-fluorescent progeny began to appear in P20, representing about 0.3% of the total infectious progeny. The proportion of the non-fluorescent virus increased with passage thereafter, becoming 99% or greater by P28 (Fig. 3C). Sequence analysis of PeGFP region of the viral genome from at least ten non-fluorescent plaques picked randomly from P20 to P28 supernatants revealed the same mutation (C289T) as observed earlier (Fig. 1C), resulting in substitution of R97C within the eGFP region of PeGFP and rendering the protein non-fluorescent. An additional mutation (G608T resulting in S203I substitution in eGFP) was also detected in these clones (Table 1). Nevertheless, the results demonstrate that once C289 in eGFP is mutated, the resultant virus gains large selective advantage and quickly increases its frequency in the population.

The rapid rate of loss of green fluorescence upon passage of the population of VSV-PeGFP in the culture supernatants of transfected cells as compared to the slow rate of loss of fluorescence of plaque-purified VSV-PeGFP could be the consequence of different evolutionary factors. It is possible that insertion of eGFP in the VSV P protein results in virus growth constraints and fitness loss. The virus then escapes from these constraints by mutating its genome as soon as it is generated from the plasmid DNA. The synergistic effects of viral growth constraint and fitness loss may drive the viral polymerase to incorporate the C289A/T mutation generating a small population of VSV-PeGFPng viruses in the culture. Due to growth advantage and fitness acquisition of the resulting nG virus, it replicates to higher levels and rapidly out-competes its fluorescent counterpart upon passage. It then predominates in the population at a faster rate due to the advantageous mutation (C289A/T) than the de novo generated variants (Dutta et al., 2008). When the population of VSV-PeGFPng increases in subsequent passages, VSV-PeGFPng has more chance to gain fitness over VSV-PeGFP as a result of larger population transmission (Novella et al., 1995). The VSV-PeGFPng then overwhelms the population and consequently, VSV-PeGFP disappears. The same trend probably occurs in the population of purely clonal VSV-PeGFP with a much slower speed, likely due to the fact that the cloned virus may have adapted to the cells to some extent through several rounds of replication. Alternatively, it is possible that the recombinant virus population after being regenerated from DNA plasmid may undergo more selective pressure compared to the clonally purified ones. The newly generated viruses from plasmid DNA must adapt to the new environment in cell culture as it was documented for VSV (Dutta et al., 2008; Gao et al., 2006). Heterologous sequences such as those of eGFP may compromise the functions or properties of the viral P protein as reported for VSV G protein containing foreign epitope insertion from HIV-1 (Schlehuber and Rose, 2004) and therefore the virus may incorporate mutation(s) to generate the protein with higher activity.

Mutation at C289 of eGFP occurs prior to mutation in M-mRFP in the context of a virus genome encoding two fluorescent fusion proteins

VSV-PeGFP-M-MmRFP virus synthesizes both PeGFP and MmRFP fusion proteins (in addition to the wild type M protein) in infected cells. Unlike PeGFP whose function is required for viral genome transcription and replication, the MmRFP fusion protein is not required during the life cycle of the virus (Das et al., 2009). Thus, the use of this dual-fluorescent virus allowed us to investigate if C289 position in eGFP is susceptible to mutation by the viral polymerase and if this mutation occurs earlier than mutation(s) appearing in the MmRFP coding region of the viral genome. Cells infected with VSV-PeGFP-M-MmRFP virus stock

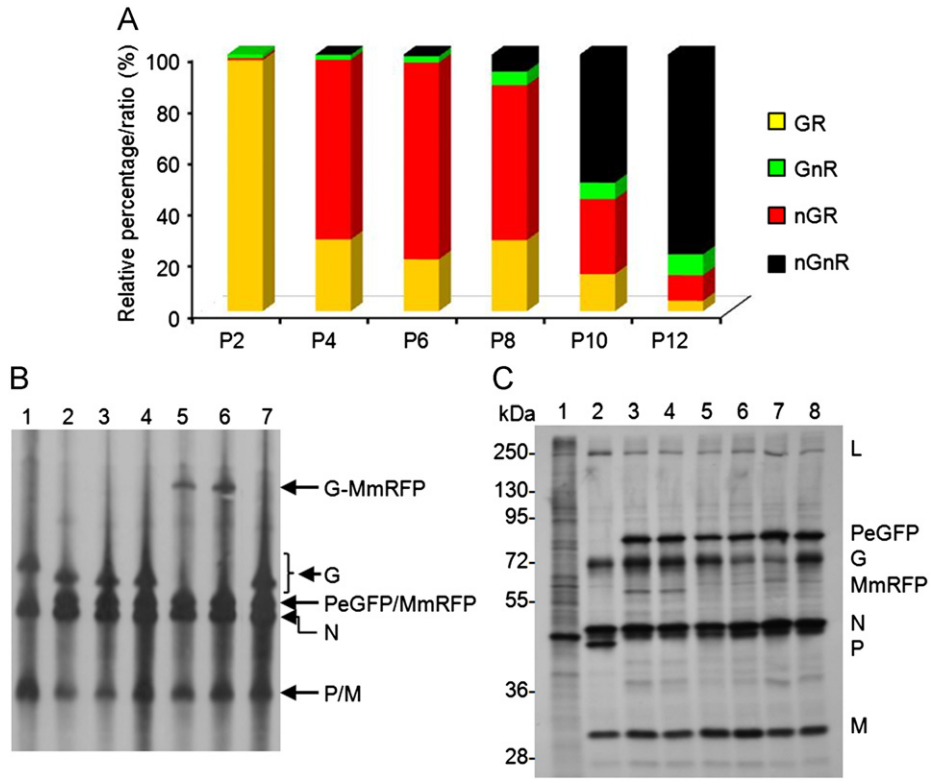

Fig. 4. Mutation at C289 of eGFP occurs first in the context of VSV-PeGFP-M-MmRFP encoding two fluorescent fusion proteins. (A) Kinetics of the emergence of viruses with all possible fluorescence phenotypes from plasmid-recovered recombinant green–red (GR) VSV-PeGFP-M-MmRFP. Culture supernatant of plasmid-recovered VSV-PeGFP-M-MmRFPgr (considered as P0) was used to infect and serially passage at an MOI of 0.01 up to passage 12. The percentage of each phenotype virus was determined by plaque counting on BHK-21 under fluorescent microscope. Histograms show the average data from two independent experiments. (B) Analysis of viral RNA in cells infected with recombinant viruses. BHK-21 was infected with 5 MOI of wt VSV (lane 1), GR (VSV-PeGFP-M-MmRFP) (lane 2), nGR (VSV-PeGFP-M-MmRFPngr) (lane 3), GnR with Stop codon in MmRFP region (VSV-PeGFP-M-MmRFP^{Stop}gnr)(lane 4), GnR with bicistronic G-MmRFP (VSV-PeGFP-M-MmRFP^{Bicis}gnr) (lane 5) and nGnR carrying C289T together with bicistronic G-MmRFP (VSV-PeGFP-M-MmRFP^{Bicis}ngnr) or with stop codon in MmRFP region (VSV-PeGFP-M-MmRFP^{Stop}ngnr) (lane 6 and 7). RNAs were labeled with ^{3}H-uridin at 5 hpi for 6 h. M and P mRNAs migrate together, PeGFP and MmRFP also have the same mobility; G mRNA in VSV-PeGFP-M-MmRFP is shortened in length compared to wt VSV, due to the insertion of MmRFP at G–L junction. (C) Analysis of viral proteins in cell infected with recombinant viruses. Infection conditions and viruses used in lane 2–8 are the same as in panel A, lane 1–7. Lane 1 contains proteins from uninfected cells. Proteins were labeled with ^{35}S-Met/Cys at 5 hpi for 4 h. Similar amounts of infected cells extracts were analyzed. Viral proteins and size markers (in kDa) are shown. (For interpretation of the references to color in this figure legend, the reader is referred to the web version of this article.)

recovered from transfected culture supernatant (without plaque purification) expressed both green and red fluorescence and greater than 99.5% of the plaques of P1 exhibited both fluorescences. However, upon passage, the green–red (GR) phenotype of the virus plaques changed and all other possible phenotypic combinations [nongreen–red (nGR), green–nonred (GnR) and nongreen–nonred (nGnR)] of the virus emerged. The relative levels of these viruses in subsequent passages changed from approximately 97.8:0.8:1.4:0 for the GR:nGR:GnR:nGnR viruses, respectively, in P2 to 28:70:1.8:0.2 in P4, indicating that the nGR phenotype dramatically increased in P4 (Fig. 4A). During these early passages (P8 or earlier), no substantial increase in GnR or nGnR virus was detected (Fig. 4A), indicating that nGR virus appears first and dominates in the population. Based on the kinetics of appearance of GR:nGR:nGnR from P2 (97.8:0.8:0) to P4 (28:70:0.2) and P12 (3:10:78) (Fig. 4A), it can be seen that the nGnR virus appears after nGR virus.

Sequence analysis revealed that the PeGFP region of the nGR virus from any of the passages possessed only the C289T mutation (Table 1), which was identified as described above. MmRFP coding region was unaltered in these viruses that displayed red fluorescence phenotype. Several mutations resulting in introduction of stop codon in M protein of MmRFP as well as mutations in the transcription termination signals upstream of the MmRFP gene that led to loss of red fluorescence were detected in GnR viruses (Table 1). Viruses with nGnR phenotype possessed a variety of mutations in addition to the mutation at C289 of eGFP (Table 1). Overall, the results suggest that C289 of eGFP was primarily mutated in the dual-fluorescent virus prior to appearance of mutations in the MmRFP region of the viral genome.

Since viruses with various phenotypes contained mutations in the transcription termination signals and/or mutations leading to stop codon in MmRFP, we examined the RNA and protein profiles in cells infected with these infectious viruses to determine the molecular basis of loss of fluorescence of these viruses. In this analysis, we examined viruses that contained mutations in the transcription termination signals and/or mutations resulting in stop codon in M region of MmRFP fusion protein. Examination of mRNA profiles showed that viruses with mutations in the transcription termination signals synthesized a bicistronic mRNA, G-MmRFP (Fig. 4B, lanes 5 and 6) with concomitant loss or undetectable levels of G and MmRFP mRNAs. Examination of virally encoded proteins in infected cells revealed that viruses with stop codon in MmRFP and/or with mutations in the transcription termination signals did not synthesize detectable levels of MmRFP fusion protein (Fig. 4C, lanes 5–8) compared to the wt VSV-PeGFP-M-MmRFP and VSV-PeGFP-M-MmRFPngr (Fig. 4C, lanes 3–4). The levels of G protein in cells infected with viruses that synthesized the bicistronic mRNA was lower (Fig. 4C, lanes 6 and 7). Importantly, in all these virus-infected cells, full-length PeGFP fusion protein was synthesized (Fig. 4C, lanes 3–8) independent of its fluorescence phenotype.

Insertion of stop codons or alterations of the transcription regulatory sequences upstream of the inserted gene has been shown to be the predominant mechanisms employed by VSV to eliminate the expression of heterologous genes inserted at the viral gene junctions (Quinones-Kochs et al., 2001; Wertz et al., 2002). The results presented here using recombinant VSVs having different genomic backgrounds further reconfirm these observations. However, with the use of VSV encoding two different fluorescent proteins, it appears that the viral polymerase first incorporates mutation(s) to generate virus with greater fitness advantage and then incorporates mutation to eliminate expression of genes inserted at the gene junction.

PeGFPng exhibits increased activity in P functions compared to PeGFP

Results from growth kinetics and competition experiments suggested that VSV-PeGFPng exhibited growth advantage and fitness gain over VSV-PeGFP virus. Therefore, we hypothesized that PeGFP fusion protein containing the R97S/C mutation may possess increased activity as a subunit of the viral polymerase. To test this hypothesis, we examined the activity of PeGFPng fusion protein and compared to that of PeGFP in VSV genome replication and transcription. The PeGFPng mutant coding sequence was cloned under T7 RNA polymerase promoter in pGEM3 vector and the ability of PeGFPngR97S protein in supporting replication of VSV DI particle RNA or transcription of a VSV minireplicon was compared to that of PeGFP. Cells were infected with vTF7-3 and subsequently transfected plasmids encoding N, L, and PeGFP, PeGFPng or empty vector. For replication assay, the cells were then infected with DI particles and radiolabeled. The radiolabeled RNAs were immunoprecipitated with anti-N antibody and analyzed as described previously (Pattnaik and Wertz, 1990). For transcription analysis, the cells were co-transfected with a minireplicon-encoding plasmid and the transcription products were radiolabeled and analyzed as before (Hwang et al., 1998). Results show that the PeGFPngR97S protein exhibits approximately three-fold higher activity in replication (Fig. 5A) as compared to the wt PeGFP protein. A similar increased activity in transcription was also observed for the mutant protein as compared to the wt protein (Fig. 5B). Under these experimental conditions, both proteins were expressed at similar levels in transfected cells (Fig. 5A and B). Since full-genome sequencing of the VSV-PeGFP and VSV-PeGFPng viruses revealed no sequence alterations other than the C289A (R97S) change, the results suggest that the higher growth and competitiveness of VSV-PeGFPng virus is primarily due to the relatively increased activity of PeGFPng fusion protein in viral genome transcription and replication as compared to PeGFP.

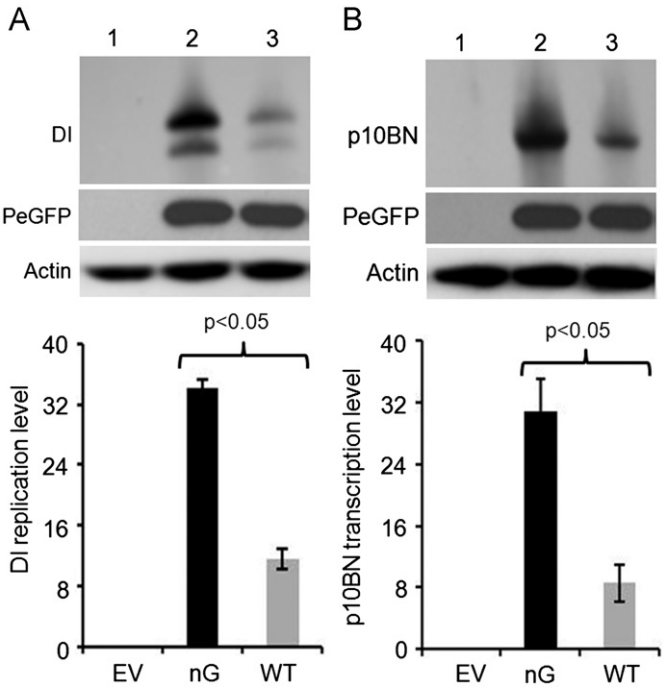

Fig. 5. Replication and transcription activity of PeGFPngR97S mutant protein. (A) DI particle RNA replication. BHK-21 cells were infected with vTF7-3 and co-transfected with plasmids encoding VSV N, L, and PeGFP (*WT*), PeGFPngR97S (nG) or pGEM3 empty vector (EV). At 10–12 hpt, cells were infected with DI particles, followed by labeling with ^{3}H-uridine for 12 h. Labeled RNAs were immunoprecipitated by anti-N antibody (1:100), separated on urea–agarose gel and detected by fluorography (A, top panel). The products were detected as a doublet representing the +ve and −ve sense DI RNA replication products. Histogram (bottom panel) shows the quantitative levels of DI replication products. Error bars represent the standard error of mean from 3 independent experiments. (B) Transcription of VSV minigenome. 10 μg of p10BN encoding a VSV minireplicon was co-transfected with pN, pL, and pPeGFP (WT), pPeGFPngR97S (nG) or pGEM3 empty vector (EV). At 8–10 hpt, cells were labeled with ^{3}H-uridine for 12 h in the presence of actinomycin D. Labeled transcription products were extracted and analyzed by electrophoresis and detected as in A (top panel). Histogram (bottom panel) shows the quantitative levels of transcription products. Error bars represent the standard error of mean from 3 independent experiments. Expression level of PeGFP (WT) or PeGFPngR97S (nG) in the transfected cells was examined by Western blotting. Levels of β-actin served as loading control.

Conclusions

The following conclusions can be derived from the results presented here. (1) The VSV polymerase specifically mutates C289 of eGFP in the context of PeGFP fusion gene to either an A or T residue. This leads to amino acid substitution R97S/C in eGFP and loss of fluorescence. (2) The non-fluorescent virus with R97S/C substitution gains growth advantage and fitness as compared to its fluorescent counterpart. (3) In recombinant VSV encoding two heterologous proteins, one as a fusion protein required for replication and another as a fusion protein not required for replication, the virus preferentially mutates first the fusion protein required for replication which allows the virus to gain growth advantage and fitness before mutating the other fusion protein. (4) The growth advantage of the non-fluorescent virus is due primarily to enhanced activity of the PeGFPng in viral genome transcription and replication.

Our results demonstrate that a gene of interest in the form of a fusion gene can be stably expressed from clonally purified VSV stock for at least twenty passages. VSV encoding different fluorescent proteins could be further used in evolutionary studies for better understanding of viral adaptability, gain/loss of fitness, growth capacity and stability of inserted genes in recombinant VSVs carrying foreign genes.

Materials and methods

Cell culture, viruses, antibodies, and reagents

Baby hamster kidney (BHK-21) monolayer cells were maintained in MEM supplemented with 5% FBS and 1 × PKS antibiotics (penicillin, 100 units/ml; kanamycin, 20 units/ml; and streptomycin, 20 units/ml). Stocks of recombinant vaccinia virus vTF7-3 (Fuerst et al., 1986) was prepared as described before (Hwang et al., 1998). Indiana strain of wild type VSV and defective interfering particles (DI-T) of wt VSV were prepared as previously described (Pattnaik and Wertz, 1990). Plasmids encoding VSV and its derivatives with fluorescent proteins have been described

earlier (Das et al., 2006; Das et al., 2009; Lawson et al., 1995). Rabbit anti-VSV P polyclonal antibody has been described before (Das and Pattnaik, 2005). Anti-VSV N (10G4) monoclonal antibodies were kindly provided by Dr. D. Lyles.

Plasmid constructs and virus recovery

pGEM3 was used for cloning of PeGFP sequences derived from various recombinant viruses. Viral genomic RNAs from culture supernatants were used for reverse transcription-polymerase chain reaction (RT-PCR) amplification of PeGFP region using P(+) and P(−) primers (Table 2). The amplified DNAs are then cloned into pGEM3 vector using EcoRV restriction site. The authentic sequence of the PeGFP clones was confirmed by nucleotide sequencing. Plasmids pN, pL, and p10BN encoding the N, L proteins or the transcription-competent minireplicon have been described previously (Hwang et al., 1998; Pattnaik et al., 1992). Cells were transfected with plasmid DNAs using Lipofectamine2000 (Invitrogen) as per manufacturer's protocol. Virus recovery and identification of recovered viruses were conducted as previously described (Das and Pattnaik, 2004).

Isolation and amplification of clonally pure virus stocks and growth kinetics analysis

Single plaques from VSV-PeGFP, VSV-eGFP, VSV-PeGFP-M-MmRFP viruses and their mutant derivatives were selected under fluorescence microscope and isolated using a sterile Pasteur pipette. Virus particles in the agarose plug were placed in virus growth medium (DMEM containing 2% fetal bovine serum and 1X PKS) and were frozen at −80 °C. To prepare clonally pure virus stocks, the thawed growth medium containing virus plaque was used as inoculum to infect a monolayer of BHK-21 cells and virus titers in the supernatants were determined by plaque assay. Growth kinetics of all viruses used in this study were determined by infection at MOI of 5 (for single-step growth) and 0.01 (for multi-step growth) following the protocol described before (Das and Pattnaik, 2004).

Virus passaging, fitness determination and calculation of fitness gain

Fitness of VSV-PeGFP and VSV-PeGFPng was determined via competition assay. Viruses were mixed together at the ratio of 1:1 and this mixture (passage 0, P0) was allowed to co-infect BHK-21 cell monolayer at an MOI of 0.01. Infection of cells with individual viruses at the same MOI was also carried out in parallel for mono-infections. At 16 h post infection (hpi), supernatant was collected and designated as P1 and virus titers were determined. The P1 virus was then used to infect new BHK-21 cell monolayer at same MOI of 0.01 to produce P2. The process was repeated to produce P5 viruses. Similarly, the competition assay was also performed at an MOI of 5 in which the supernatant of each passage was harvested at 8 hpi. The titer of each virus in competition or

Table 2
Primers used in this study.

Primer name	Primer nucleotide sequences	Used for
MfeI-N-For	AGAAGACAATTGGCAAGTATGC	Amplification and sequencing of the PeGFP region
M2481Rev	GTGTAGACTCATACAAGAC	
eGFP188-Rev	GTCACGAGGGTGGGCCAGGG	
P2600For	ATTATGAAGGAGCGCCAG	
G-4518-For	GTTCTCCGAGTTGGTA	Amplification and sequencing of the MmRFP or eGFP region at G–L junction
L-5093-Rev	CTGCCTCTTTGTCCACTTC	
Le(+) For	ACGAAGACAAACAAACCATTATTA	Amplification and sequencing of the fragment spanning nucleotides 1–2500 of full-length VSV genome
N440For	CACAAATGCCTGAATACAG	
N533Rev	GCTGGAAGACCGTGTTCTCC	
MfeI-N-For	AGAAGACAATTGGCAAGTATGC	
eGFP188-Rev	GTCACGAGGGTGGGCCAGGG	
P2600For	ATTATGAAGGAGCGCCAG	
P1430R	AACTCTATGAGTGCTTGAAAACAC	
P(−)	ATATATCTGCAGATATCTGTTACTTTTTTTCATAGTCTACAGAGAATATTTG	
M2481Rev	GTGTAGACTCATACAAGAC	
VSV2160For	GTACAATCAGGCGAGAGTCA	Amplification and sequencing of the fragment spanning nucleotides 2180–4670 of full-length VSV genome
VSV2523For	GATCACATGTACATCGGAATG	
G4124For	GGAACTTGGCTGAATC	
G-NdeI Rev	CAGTGGGGCATATGTAATTG	
G4548F	GATCTCTTTGCTGCAG	
G4668Rev	GGTATCACAAGTTGATTTGG	
G-4518-For	GTTCTCCGAGTTGGTA	Amplification and sequencing of the fragment spanning nucleotides 4530–6920 of full-length VSV genome
L-StuI For	AGAATCAAGGCCTTTAGTCC	
L-DrdI Rev	AGGATGACCCCAATGTCTG	
L-5093-Rev	CTGCCTCTTTGTCCACTTC	
L-AclI Rev	GTAATTCTACAACGTTTCTCG	
L-BclI For	CACACTGATCAATTCAACCTC	Amplification and sequencing of the fragment spanning nucleotides 6730–9080 of full-length VSV genome
L-EcoRI For	TAAGTGAATTCAAATCAGGCAC	
L-825I-NotIR	AAAATGAGCTACGGTGAGAG	
L-PciI Rev	GAGTAGCTGAACATGTCCAC	
L630II-NotIR	TGATCTAGTAAGAGAAAGGAATG	
L-AseI For	AGACGGATTAATGAGAGCAAG	Amplification and sequencing of the fragment spanning nucleotides 8950–11161 of full-length VSV genome
L-BstXI For	CAAGGACTTGGGACTATTTC	
L-ScaIF	AGAAGTGGAGTACTAGAGG	
L-SalI Rev	TTTGAACTAAGTCGACCGTC	
Tr(+) Rev	ACGAAGACCACAAAACCAG	
P(+)-For	ATATATGGTACCGATATCATGGATAATCTCACAAAAGTTCGTGAG	Cloning of PeGFP fragment
P(−)	ATATATCTGCAGATATCTGTTACTTTTTTTCATAGTCTACAGAGAATATTTG	

Primer sequences are in 5′–3′ direction. Restriction enzyme sites in the primers are underlined.

mono-infection at each passage was determined by plaque assay on BHK-21 and green and nongreen plaques were counted on fluorescence microscope. Approximately 500–1000 plaques were examined for early passage virus (P0–P1) and 10^5–10^6 plaques for later passage virus (P2–P5). The data shown in this study were the average of three replicates of plaque assay. Relative fitness values (W) were calculated based on the amount of a specific VSV phenotype in a competition infection divided by the amount of the same virus resulting from a mono-infection under the same experimental conditions (Kong et al., 2008). The formulae are:

$$W_G = \frac{(Gc/Gm)}{(Gc/Gm)+(nGc/nGm)} \times 2$$

$$W_{nG} = \frac{(nGc/nGm)}{(nGc/nGm)+(Gc/Gm)} \times 2$$

where, W_{nG} and W_G represent nongreen and green virus relative fitness values; Gc and nGc represent the amount of VSV-PeGFP and VSV-PeGFPng particles, respectively, in competition infection; Gm and nGm represent the amount of VSV-PeGFP and VSV-PeGFPng particles, respectively, in mono-infection. The ratio of relative fitness value of each virus in the competition assay is measured via the fitness difference, $Wd = W_{NG}/W_G$. A value of $Wd > 1$ indicates that VSV-PeGFPng is more fit than VSV-PeGFP and a value of $Wd < 1$ indicates that VSV-PeGFPng is less fit than VSV-PeGFP.

To determine the kinetics of non-fluorescent virus emergence, initially recovered culture supernatants (passage 0 (P0)) of VSV-eGFP, VSV-PeGFP-M-MmRFP, and VSV-PeGFP as well as purely clonal VSV-PeGFP from an isolated plaque (P0) were allowed to infect BHK-21 cell monolayer at an MOI of 0.01. At 16–20 hpi, supernatant was collected and designated P1. The P1 then was used to infect new BHK-21 cell monolayer at same MOI of 0.01 to produce P2 and subsequent passages were performed similarly.

RNA replication and transcription assays

These assays have been described previously (Hwang et al., 1998; Pattnaik and Wertz, 1990). The ability of PeGFP and its mutant forms in supporting VSV RNA replication was determined by using the DI RNA replication assay (Pattnaik and Wertz, 1990). Briefly, cells infected with vTF7-3 (Fuerst et al., 1986) were transfected with plasmid encoding N, L, and PeGFP, PeGFPng or empty vector for 10–12 h. Then the cells were infected with DI particles of VSV, radiolabeled with 50 μCi/ml ^{3}H-uridine for 12 h. Radiolabeled RNAs were immunoprecipitated with anti-N antibody and analyzed by electrophoresis as described before (Pattnaik and Wertz, 1990). Transcription activity of PeGFP and its mutant was determined using the VSV minireplicon as described previously (Hwang et al., 1998). Western blot to determine the expression level of PeGFP and its mutant was performed as described previously (Dinh et al., 2011) using anti-VSV P polyclonal antibody (1:1000) followed by goat anti-rabbit immunoglobulin (IgG)-horseradish peroxidase (1:4000).

Examination of viral RNA and viral proteins

BHK-21 cell monolayer was infected with viruses at an MOI of 5 for 4 h. For RNA labeling, cells were treated with actinomycin D (15 μg/ml) to inhibit cellular transcription for 1 h before incubated in medium containing 50 μCi/ml ^{3}H-uridine in the presence of actinomycin D for another 6 h. Cells were then lysed in Trizol (Invitrogen) for RNA extraction. Radiolabeled RNAs were analyzed by electrophoresis and detected by fluorography. For protein labeling, cells were starved in methionine/cysteine-free medium (Invitrogen) for 1 h followed by 4 h labeling with 50 μCi/ml of ^{35}S Met/Cys (NEN Life Sciences, MA). Cells were lysed in RIPA buffer and the labeled proteins were analyzed by 10% SDS-PAGE and detected by fluorography (Das et al., 2010).

Reverse transcriptase-polymerase chain reaction (RT-PCR) and sequencing

Viral RNAs from the viruses in the culture supernatant were extracted by TRIzol LS (Invitrogen) as per manufacturer's protocol. RT reactions were performed using Superscript III RT (Invitrogen), followed by PCR with Faststart high fidelity PCR system (Roche) as previously described (Dinh et al., 2011). Nucleotide sequencing of PeGFP, MmRFP, eGFP regions from viruses shown in Table 1 as well the PCR amplified fragments spanning the entire genome of VSV-PeGFP and VSV-PeGFPngR97S viruses isolated from P0 of transfected culture supernatant was performed by Eurofins MWG Operon (Huntsville, AL 35805). Primers used in RT-PCR and sequencing are shown in Table 2.

Statistical analysis

Differences of viral titers in growth comparison and in competition assays were analyzed using the MIXED procedure (SAS Inst. Inc., Cary, NC). Statistical model included Treatment as a fixed effect. All means are presented as least-squares means ($\pm$SEM). A value of $p < 0.05$ was considered to represent statistical significance.

Acknowledgments

We thank Z. H. Gill for excellent assistance in the laboratory. This work was supported in part by National Institutes of Health grant R01 AI34956.

References

Barber, G.N., 2005. VSV-tumor selective replication and protein translation. Oncogene 24, 7710–7719.
Barondeau, D.P., Putnam, C.D., Kassmann, C.J., Tainer, J.A., Getzoff, E.D., 2003. Mechanism and energetics of green fluorescent protein chromophore synthesis revealed by trapped intermediate structures. Proc. Natl. Acad. Sci. USA 100, 12111–12116.
Clarke, D.K., Duarte, E.A., Elena, S.F., Moya, A., Domingo, E., Holland, J., 1994. The red queen reigns in the kingdom of RNA viruses. Proc. Natl. Acad. Sci. USA 91, 4821–4824.
Dalton, K.P., Rose, J.K., 2001. Vesicular stomatitis virus glycoprotein containing the entire green fluorescent protein on its cytoplasmic domain is incorporated efficiently into virus particles. Virology 279, 414–421.
Das, P.B., Dinh, P.X., Ansari, I.H., de Lima, M., Osorio, F.A., Pattnaik, A.K., 2010. The minor envelope glycoproteins GP2a and GP4 of porcine reproductive and respiratory syndrome virus interact with the receptor CD163. J. Virol. 84, 1731–1740.
Das, S.C., Pattnaik, A.K., 2004. Phosphorylation of vesicular stomatitis virus phosphoprotein P is indispensable for virus growth. J. Virol. 78, 6420–6430.
Das, S.C., Pattnaik, A.K., 2005. Role of the hypervariable hinge region of phosphoprotein P of vesicular stomatitis virus in viral RNA synthesis and assembly of infectious virus particles. J. Virol. 79, 8101–8112.
Das, S.C., Nayak, D., Zhou, Y., Pattnaik, A.K., 2006. Visualization of intracellular transport of vesicular stomatitis virus nucleocapsids in living cells. J. Virol. 80, 6368–6377.
Das, S.C., Panda, D., Nayak, D., Pattnaik, A.K., 2009. Biarsenical labeling of vesicular stomatitis virus encoding tetracysteine-tagged m protein allows dynamic imaging of m protein and virus uncoating in infected cells. J. Virol. 83, 2611–2622.
Dinh, P.X., Beura, L.K., Panda, D., Das, A., Pattnaik, A.K., 2011. Antagonistic effects of cellular poly(C) binding proteins on vesicular stomatitis virus gene expression. J. Virol. 85, 9459–9471.
Domingo, E., Briebicher, C.K., Holland, J.J., Eigen, M., 2001. In Quasispecies and RNA Virus Evolution: Principles and Consequences, 2001. Landes Bioscience, Georgetown.
Domingo, E., Sabo, D., Taniguchi, T., Weissmann, C., 1978. Nucleotide sequence heterogeneity of an RNA phage population. Cell 13, 735–744.
Duarte, E., Clarke, D., Moya, A., Domingo, E., Holland, J., 1992. Rapid fitness losses in mammalian RNA virus clones due to Muller's ratchet. Proc. Natl. Acad. Sci. USA 89, 6015–6019.

Dutta, R.N., Rouzine, I.M., Smith, S.D., Wilke, C.O., Novella, I.S., 2008. Rapid adaptive amplification of preexisting variation in an RNA virus. J. Virol. 82, 4354–4362.
Elena, S.F., Gonzalez-Candelas, F., Novella, I.S., Duarte, E.A., Clarke, D.K., Domingo, E., Holland, J.J., Moya, A., 1996. Evolution of fitness in experimental populations of vesicular stomatitis virus. Genetics 142, 673–679.
Fang, Y., Rowland, R.R., Roof, M., Lunney, J.K., Christopher-Hennings, J., Nelson, E.A., 2006. A full-length cDNA infectious clone of North American type 1 porcine reproductive and respiratory syndrome virus: expression of green fluorescent protein in the Nsp2 region. J. Virol. 80, 11447–11455.
Fang, Y., Christopher-Hennings, J., Brown, E., Liu, H., Chen, Z., Lawson, S.R., Breen, R., Clement, T., Gao, X., Bao, J., Knudsen, D., Daly, R., Nelson, E., 2008. Development of genetic markers in the non-structural protein 2 region of a US type 1 porcine reproductive and respiratory syndrome virus: implications for future recombinant marker vaccine development. J. Gen. Virol. 89, 3086–3096.
Fuerst, T.R., Niles, E.G., Studier, F.W., Moss, B., 1986. Eukaryotic transient-expression system based on recombinant vaccinia virus that synthesizes bacteriophage T7 RNA polymerase. Proc. Natl. Acad. Sci. USA 83, 8122–8126.
Gao, Y., Whitaker-Dowling, P., Watkins, S.C., Griffin, J.A., Bergman, I., 2006. Rapid adaptation of a recombinant vesicular stomatitis virus to a targeted cell line. J. Virol. 80, 8603–8612.
Gause, G.F., Laiko, A.V., Bibikova, M.V., Kusovkova, L.I., Selesneva, T.I., Dudnik, Y.V., 1971. Mutants with altered DNA base composition in Bacterium paracoli—the evidence from a marker. Z. Allg. Mikrobiol. 11, 91–95.
Geisbert, T.W., Bausch, D.G., Feldmann, H., 2010. Prospects for immunisation against Marburg and Ebola viruses. Rev. Med. Virol. 20, 344–357.
Heiber, J.F., Xu, X.X., Barber, G.N., 2011. Potential of vesicular stomatitis virus as an oncolytic therapy for recurrent and drug-resistant ovarian cancer. Chin. J. Cancer 30, 805–814.
Hwang, L.N., Englund, N., Pattnaik, A.K., 1998. Polyadenylation of vesicular stomatitis virus mRNA dictates efficient transcription termination at the intercistronic gene junctions. J. Virol. 72, 1805–1813.
Kim, D.Y., Calvert, J.G., Chang, K.O., Horlen, K., Kerrigan, M., Rowland, R.R., 2007. Expression and stability of foreign tags inserted into nsp2 of porcine reproductive and respiratory syndrome virus (PRRSV). Virus Res. 128, 106–114.
Kong, X., West, J.T., Zhang, H., Shea, D.M., M'Soka, T., Wood, C., J., 2008. The human immunodeficiency virus type 1 envelope confers higher rates of replicative fitness to perinatally transmitted viruses than to nontransmitted viruses. J. Virol. 82, 11609–11618.
Kuge, S., Kawamura, N., Nomoto, A., 1989. Strong inclination toward transition mutation in nucleotide substitutions by poliovirus replicase. J. Mol. Biol. 207, 175–182.
Lawson, N.D., Stillman, E.A., Whitt, M.A., Rose, J.K., 1995. Recombinant vesicular stomatitis viruses from DNA. Proc. Natl. Acad. Sci. USA 92, 4477–4481.
Lichty, B.D., Power, A.T., Stojdl, D.F., Bell, J.C., 2004. Vesicular stomatitis virus: re-inventing the bullet. Trends Mol. Med. 10, 210–216.
McKenna, P.M., McGettigan, J.P., Pomerantz, R.J., Dietzschold, B., Schnell, M.J., 2003. Recombinant rhabdoviruses as potential vaccines for HIV-1 and other diseases. Curr. HIV Res. 1, 229–237.
Moya, A., Elena, S.F., Bracho, A., Miralles, R., Barrio, E., 2000. The evolution of RNA viruses: A population genetics view. Proc. Natl. Acad. Sci. USA 97, 6967–6973.
Muller, H.J., 1964. The Relation of Recombination to Mutational Advance. Mutat. Res. 106, 2–9.
Novella, I.S., 2003. Contributions of vesicular stomatitis virus to the understanding of RNA virus evolution. Curr. Opin. Microbiol. 6, 399–405.
Novella, I.S., Ball, L.A., Wertz, G.W., 2004a. Fitness analyses of vesicular stomatitis strains with rearranged genomes reveal replicative disadvantages. J. Virol. 78, 9837–9841.
Novella, I.S., Reissig, D.D., Wilke, C.O., 2004b. Density-dependent selection in vesicular stomatitis virus. J. Virol. 78, 5799–5804.
Novella, I.S., Duarte, E.A., Elena, S.F., Moya, A., Domingo, E., Holland, J.J., 1995. Exponential increases of RNA virus fitness during large population transmissions. Proc. Natl. Acad. Sci. USA 92, 5841–5844.
Ormo, M., Cubitt, A.B., Kallio, K., Gross, L.A., Tsien, R.Y., Remington, S.J., 1996. Crystal structure of the Aequorea victoria green fluorescent protein. Science 273, 1392–1395.
Pattnaik, A.K., Wertz, G.W., 1990. Replication and amplification of defective interfering particle RNAs of vesicular stomatitis virus in cells expressing viral proteins from vectors containing cloned cDNAs. J. Virol. 64, 2948–2957.
Pattnaik, A.K., Ball, L.A., LeGrone, A.W., Wertz, G.W., 1992. Infectious defective interfering particles of VSV from transcripts of a cDNA clone. Cell 69, 1011–1020.
Pfeiffer, J.K., Kirkegaard, K., 2006. Bottleneck-mediated quasispecies restriction during spread of an RNA virus from inoculation site to brain. Proc. Natl. Acad. Sci. USA 103, 5520–5525.
Quinones-Kochs, M.I., Schnell, M.J., Buonocore, L., Rose, J.K., 2001. Mechanisms of loss of foreign gene expression in recombinant vesicular stomatitis viruses. Virology 287, 427–435.
Ruedas, J.B., Perrault, J., 2009. Insertion of enhanced green fluorescent protein in a hinge region of vesicular stomatitis virus L polymerase protein creates a temperature-sensitive virus that displays no virion-associated polymerase activity in vitro. J. Virol. 83, 12241–12252.
Schlehuber, L.D., Rose, J.K., 2004. Prediction and identification of a permissive epitope insertion site in the vesicular stomatitis virus glycoprotein. J. Virol. 78, 5079–5087.
Schneider, W.L., Roossinck, M.J., 2000. Evolutionarily related Sindbis-like plant viruses maintain different levels of population diversity in a common host. J. Virol. 74, 3130–3134.
Steinhauer, D.A., de la Torre, J.C., Holland, J.J., 1989. High nucleotide substitution error frequencies in clonal pools of vesicular stomatitis virus. J. Virol. 63, 2063–2071.
van Valen, L., 1973. A new evolutionary law. Evol. Theory 1, 1–30.
Vignuzzi, M., Stone, J.K., Arnold, J.J., Cameron, C.E., Andino, R., 2006. Quasispecies diversity determines pathogenesis through cooperative interactions in a viral population. Nature 439, 344–348.
Wertz, G.W., Moudy, R., Ball, L.A., 2002. Adding genes to the RNA genome of vesicular stomatitis virus: positional effects on stability of expression. J. Virol. 76, 7642–7650.